Cui *et al*. *Complex Eng Syst* 2023;3:3
DOI: 10.20517/ces.2022.57

Complex Engineering Systems

Research Article

Open Access

Parameters optimization of electro-hydraulic power steering system based on multi-objective collaborative method

Taowen Cui[1,2], Shuaiyin Wang[1], Yuan Qu[2], Xiang Chen[2]

[1]Intelligent Vector Technology Control Lab, Chery Automobile Company Limited, Wuhu 241000, Anhui, China.
[2]School of Automotive and Transportation Engineering, Hefei University of Technology, Hefei 230041, Anhui, China.

Correspondence to: Dr. Taowen Cui, School of Automotive and Transportation Engineering, Hefei University of Technology, Hefei 230041, Anhui, China. E-mail:nuaa_ctw@126.com

How to cite this article: Cui T, Wange S, Qu Y, Chen X. Parameters optimization of electro-hydraulic power steering system based on multi-objective collaborative method. *Complex Eng Syst* 2023;3:3. http://dx.doi.org/10.20517/ces.2022.57

Received: 20 Dec 2022 **First Decision:** 19 Jan 2023 **Revised:** 3 Feb 2023 **Accepted:** 17 Feb 2023 **Published:** 9 Mar 2023

Academic Editors: Hamid Reza Karimi, Serdar Coskun **Copy Editor:** Fangling Lan **Production Editor:** Fangling Lan

Abstract

Electro-hydraulic power steering (EHPS) systems are widely used in commercial vehicles due to their adjustable power assist and energy-saving advantages. In this paper, a dynamic model of the EHPS system is developed, and quantitative expressions for three evaluation indexes, steering road feel, steering sensibility and steering energy loss, are derived for the first time. A multi-objective collaborative optimization model of the EHPS system is then established, which consists of one total system and three parallel subsystems, based on collaborative optimization theory. Considering the coupled variables of each subsystem, the total system is optimized by a multi-objective algorithm, while the subsystems are optimized by a single-objective algorithm. The optimization results demonstrate that the average frequency domain energy of the steering road feel is increased by 69.1%, the average frequency domain energy of steering sensitivity is reduced by 19.2%, and steering energy consumption is reduced by 10.8% compared to the initial value. The non-dominated sorting genetic algorithm-II (NSGA-II) shows superior comprehensive performance compared to the other two multi-objective algorithms, and the optimization performance can be further improved by setting appropriate algorithm parameters.

Keywords: Electro-hydraulic power steering, multi-objective optimization, collaborative optimization, non-dominated sorting genetic algorithm-II

1. INTRODUCTION

As the focus on driving experience increases, research into vehicle steering systems has also gained attention. Traditional hydraulic power steering (HPS) systems provide assistance torque through an engine and offer a clear road feel, but have the disadvantage of high energy consumption. Electric power steering (EPS) systems provide adjustable assistance torque through a motor and have lower energy consumption, but the power-assisted range of EPS systems is narrow, limiting their application in vehicles with heavy front axle loads. Electric-hydraulic power steering (EHPS) systems combine the advantages of both systems, providing better road feel and lower energy consumption. Thus, EHPS systems have been widely used in commercial vehicles.

In recent years, research into EHPS systems has mainly focused on the control aspect[1–6]. Neural network control algorithms have been applied to the steering assist control of EHPS systems to improve the driver's experience[7]. Kim *et al.* proposed a design method for the steering motor speed of EHPS systems based on driver perception, which improved the driver's steering road feel and eliminated the catch-up effect[8]. Lin *et al.* proposed a slip frequency control method for the steering motor of EHPS systems to effectively improve the response speed and accuracy of the steering motor[9]. Ye *et al.* simplified the EHPS system and introduced the H2/H∞ control method to control the power assistance, which improves the anti-interference performance of the steering system[10]. Hur *et al.* analyzed the characteristics of the interior permanent-magnet synchronous motor of EHPS systems and proposed precise control and real-time response control methods for the motor[11].

However, current research rarely focuses on the steering experience of EHPS systems, and the optimization of the overall EHPS system is rarely reported. The evaluation indexes of EHPS systems involve not only steering flexibility and road feel, but also steering economy and other aspects with coupled effects[12–14]. Therefore, the optimization of the EHPS system is essentially a multi-objective optimization problem (MOP).

Traditional multi-objective optimization algorithms usually set different weights for different indicators and sum them, thus transforming multi-objective optimization into single-objective optimization[15]. However, these optimization algorithms show poorer performance in solving too many optimization objectives and non-convex optimization problems, and are prone to falling into local optima[16]. As such, a number of intelligent optimization algorithms, such as non-dominated sorting genetic algorithm (NSGA) and NSGA-II, have been proposed and applied to satellite design and other fields[17,18]. Additionally, the collaborative optimization (CO) method can effectively solve complex optimization problems, with the obvious advantages of simplifying system decoupling and achieving parallel computation[19–21]. The complex optimization model is divided into several subsystems according to the optimization objectives, and the coupling variables in the subsystems are coordinated by the consistency constraint[22]. This is convenient for concurrent design, which is consistent with the modern industrial design structure[23–25].

In this paper, steering road feel, steering sensitivity, and steering energy loss are taken as evaluation indexes. Considering the coupling factors of each subsystem, the multi-objective collaborative optimization method of the EHPS system is explored.

The rest of the paper is organized as follows. The dynamic model of the EHPS system is established in Section 2, and the three evaluation indexes of the steering system are derived for the first time. Section 3 establishes the multi-objective collaborative optimization model of the EHPS system and shows the multi-objective optimization results. Conclusions are given in Section 4.

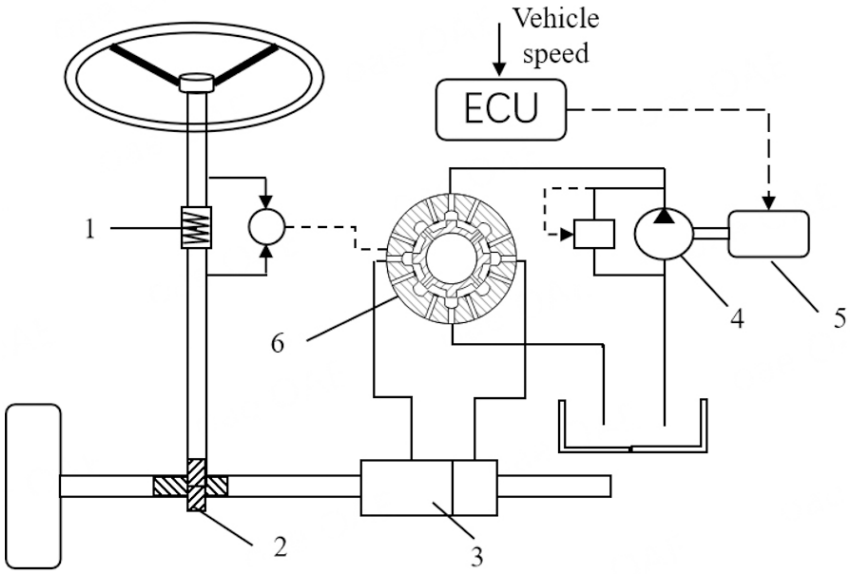

Figure 1. Structure of EHPS system. 1-Torque sensor; 2-rack and pinion;3-hydraulic cylinder; 4- hydraulic pump; 5-drive motor; 6-rotary valve.

2. SYSTEM DYNAMIC MODEL

The EHPS system consists of two parts: mechanical and hydraulic. The mechanical part includes a sequential connection of the steering wheel, steering column, rack and pinion, *etc*. The hydraulic part includes the oil tank, hydraulic pump, drive motor, rotary valve, and hydraulic cylinder. According to the vehicle speed and steering wheel torque, the drive motor drives the hydraulic pump at a certain speed to supply oil to the rotary valve and form a pressure difference on both sides. This pressure difference then provides adjustable assistance for the steering system through the hydraulic cylinder.

The EHPS system structure is shown in Figure 1.

2.1. Steering model

The dynamics model of the EHPS system can be expressed as follows, which includes the steering wheel model, drive motor model, rack and pinion model, and steering resistance torque model [2,8].

$$\begin{cases} J_{sw}\ddot{\theta}_{sw} + B_{sw}\dot{\theta}_{sw} = T_{sw} - T_s \\ J_m\frac{d\omega}{dt} + B_d\omega = T_m - T_c \\ m_o\ddot{x}_o + B_o\dot{x}_o = F_{ss} + F_h - F_r \\ T_r = \frac{2dk_1}{n_1}\left(\frac{a\omega_r}{u} + E_1\phi + \beta - \delta\right) \end{cases} \tag{1}$$

where

$$\begin{cases} F_h = A_p\left(\frac{\rho}{8\left(C_qA_2\right)^2}\left(Q_s - A_p\frac{dx_r}{dt}\right)^2 - \frac{\rho}{8\left(C_qA_1\right)^2}\left(Q_s + A_p\frac{dx_r}{dt}\right)^2\right) \\ q = 2p_b\left[\pi\left(R_2^2 - R_1^2\right) - \left(R_2 - R_1\right)Zt\right] \\ p_S = \frac{\rho}{8\left(C_qA_1\right)^2}\left(Q_s + A_p\frac{dx_r}{dt}\right)^2 + \frac{\rho}{8\left(C_qA_2\right)^2}\left(Q_s - A_p\frac{dx_r}{dt}\right)^2 \\ T_c = \frac{qP_s}{2\pi k_p} \end{cases}$$

2.2. Steering performance indexes

Considering the performance requirements of the EHPS system, steering road feel, steering sensibility, and steering energy loss are taken as the evaluation indexes. The quantitative formulas of the three evaluation indexes are derived as follows.

2.2.1 Steering road feel

In this paper, steering road feel is defined as a transfer function from steering resistance torque T_r to steering wheel torque T_{sw}, which reflects the efficiency of transmitting torque fluctuations from the road surface to the driver. Besides, the steering wheel angle θ_{sw} is defined as 0 to reduce a degree of freedom and facilitate the analysis of the steering system.

It is assumed that the torque sensor can be simplified as a torsion bar spring, and the measured value of the torque sensor could be computed by

$$T_s = K_s\left(\theta_{sw} - \theta_p\right) = -K_s\theta_p \tag{2}$$

where T_{sw} is torque obtained by torque sensor.

According to the current control strategy, the current can be given by

$$I = KT_s \tag{3}$$

The torque T_m provided by the motor can be given by

$$T_m = -K_aKK_s\theta_p \tag{4}$$

Where K_a is the torque coefficient of the motor, K is power gain coefficient.

According to (1)-(4), steering road feel can be computed as follows.

$$E(s) = \frac{T_{sw}(s)}{T_r(s)} = \frac{K_sq}{X_1s^2 + Y_1s + Z_1} \tag{5}$$

where

$$\begin{cases} X_1 = \mathrm{m}_r r_p^2 q + n_2 J_m A_p r_p \\ Y_1 = B_r q r_p^2 + n_2 B_m A_p r_p + \frac{\rho q^2 n \eta_v A_p^2 r_p^2}{2C_q^2 A_1^2} \\ Z_1 = A_p r_p K K_a K_s + q K_{TT} \end{cases}$$

Generally, the effective road information frequency domain range is 0-40 Hz. Thus, steering road feel is measured by its average frequency power within this range.

$$S_c = \frac{1}{2\pi\omega_0}\int_0^{\omega_0} |E(j\omega)|^2 d\omega \tag{6}$$

2.2.2 Steering sensibility

Steering sensitivity reflects the response speed of a vehicle to steering action and has an important impact on vehicle safety at high speed.

The vehicle three degree of freedom differential equation can be described as[17]

$$\begin{cases} I_z\dot{\omega}_r - I_x\ddot{\phi} = N_r\omega_r + N_\beta\beta + N_\phi\phi + N_\delta\delta \\ mu\left(\omega_r + \dot{\beta}\right) - m_sh\ddot{\phi} = Y_r\omega_r + Y_\beta\beta + Y_\phi\phi + Y_\delta\delta \\ I_x\ddot{\phi} - m_su\left(\omega_r + \dot{\beta}\right)h - I_x\dot{\omega}_r = L_p\dot{\phi} + L_\phi\phi \end{cases} \tag{7}$$

where

$$
\begin{aligned}
&N_r = -2\frac{a^2k_1+b^2k_2}{u} && N_\beta = -2ak_1 + 2bk_2\\
&N_\phi = -2aE_1k_1 + 2bE_2k_2 && N_\delta = 2ak_1\\
&Y_r = -2\frac{k_1a-k_2b}{u} && Y_\beta = -2\left(k_1+k_2\right)\\
&Y_\phi = -2k_1E_1 - 2k_2E_2 && Y_\delta = 2k_1\\
&L_\phi = -[2k_1E_1h + 2k_2E_2h + 2(C_{21}+C_{23}+\tfrac{C_{a1}+C_{a2}}{d^2})d^2 - m_sgh]\\
&L_p = -2\left(D_{21}+D_{23}\right)d^2
\end{aligned}
$$

The following formula can be obtained by Laplace transformation of the above formula

$$
\begin{cases}
\frac{\omega_r(s)}{\delta(s)} = \frac{A_3s^3+A_2s^2+A_1s+A_0}{B_4s^4+B_3s^3+B_2s^2+B_1s+B_0}\\
\frac{\beta(s)}{\delta(s)} = \frac{F_3s^3+F_2s^2+F_1s+F_0}{B_4s^4+B_3s^3+B_2s^2+B_1s+B_0}\\
\frac{\phi(s)}{\delta(s)} = \frac{H_2s^2+H_1s+H_0}{B_4s^4+B_3s^3+B_2s^2+B_1s+B_0}
\end{cases}
\tag{8}
$$

where

$$
\begin{aligned}
A_3 &= -muI_xN_\delta + h^2um_s^2N_\delta - huI_{xz}m_sY_\delta\\
A_2 &= muL_pN_\delta + I_xN_\delta Y_\beta - I_xN_\beta Y_\delta\\
A_1 &= muL_\phi N_\delta - L_pN_\delta Y_\beta + L_pN_\beta Y_\delta - \text{ hum }_sN_\phi Y_\delta + h_sN_\delta Y_\phi\\
A_0 &= -L_\phi N_\delta Y_\beta + L_\phi N_\beta Y_\delta\\
B_4 &= muI_{xz}^2 - muI_xI_z + h^2uI_zm_s^2\\
B_3 &= muI_zL_p + muI_xN_r - h^2um_s^2N_r + hI_{xz}m_sN_\beta + huI_{xz}m_sY_r - I_{xz}^2Y_\beta + I_xI_zY_\beta\\
B_2 &= muI_zL_\phi - muL_pN_r - muI_xN_\beta + h^2um_s^2N_\beta + muI_{xz}N_\phi + I_xN_\beta Y_r - I_zL_pY_\beta\\
&\quad -huI_{xz}m_sY_\beta - I_xN_rY_\beta + huI_zm_sY_\phi\\
B_1 &= -muL_\phi N_r + muL_pN_\beta - L_pN_\beta Y_r + h^{hum_s}N_\phi Y_r - I_zL_\phi Y_\beta + L_pN_rY_\beta - I_{xz}N_\phi Y_\beta\\
&\quad - \text{ hum }_sN_rY_\phi + I_{xz}N_\beta Y_\phi\\
B_0 &= muL_\phi N_\beta - L_\phi N_\beta Y_r + L_\phi N_rY_\beta - \text{ hum }_sN_\phi Y_\beta + \text{ hum }_sN_\beta Y_\phi\\
F_3 &= -hI_{xz}m_sN_\delta + I_{xz}^2Y_\delta - I_xI_zY_\delta\\
F_2 &= muI_xN_\delta - h^2um_s^2N_\delta - I_xN_\delta Y_r + I_zL_pY_\delta + huI_{xz}m_sY_\delta + I_xN_rY_\delta\\
F_1 &= -muL_pN_\delta + L_pN_\delta Y_r + I_zL_\phi Y_\delta - L_pN_rY_\delta + I_{xz}N_\phi Y_\delta - I_{xz}N_\delta Y_\phi\\
F_0 &= -muL_\phi N_\delta + L_\phi N_\delta Y_r - L_\phi N_rY_\delta + hum_sN_\phi Y_\delta - hum_sN_\delta Y_\phi\\
H_2 &= -muI_{xz}N_\delta - huI_zm_sY_\delta\\
H_1 &= -\text{ hum }_sN_\delta Y_r + I_{xz}N_\delta Y_\beta + \text{ hum }_sN_rY_\delta - I_{xz}N_\beta Y_\delta\\
H_0 &= \text{ hum }_sN_\delta Y_\beta - \text{ hum }_sN_\beta Y_\delta
\end{aligned}
$$

According to Formula (1) and (8), the transfer function from the rotation angle of steering wheel $\theta_{sw}(s)$ to the rotation angle of front wheel $\delta(s)$ can be expressed as

$$
\frac{\delta(s)}{\theta_{sw}(s)} = \frac{A_pr_pKK_aK_s + K_sq}{X_2s^2 + Y_2s + Z_2 + \frac{q2dk_1}{n_2}\left(\frac{a}{u}\frac{w_r(s)}{\delta(s)} + \frac{\beta(s)}{\delta(s)} + E_1\frac{\phi(s)}{\delta(s)}\right)}
\tag{9}
$$

where

$$
\begin{cases}
\mathrm{X}_2 = \mathrm{m}_rr_p^2qn_1 + n_1n_2J_mA_pr_p\\
Y_2 = \left(B_rqr_p^2 + n_2B_mA_pr_p + \frac{\rho q^2n\eta_vA_p^2r_p^2}{2C_q^2A_1^2}\right)n_1\\
Z_2 = \left(A_pr_pKK_aK_s + K_sq\right)n_1 - \frac{2qdk_1}{n_1}
\end{cases}
$$

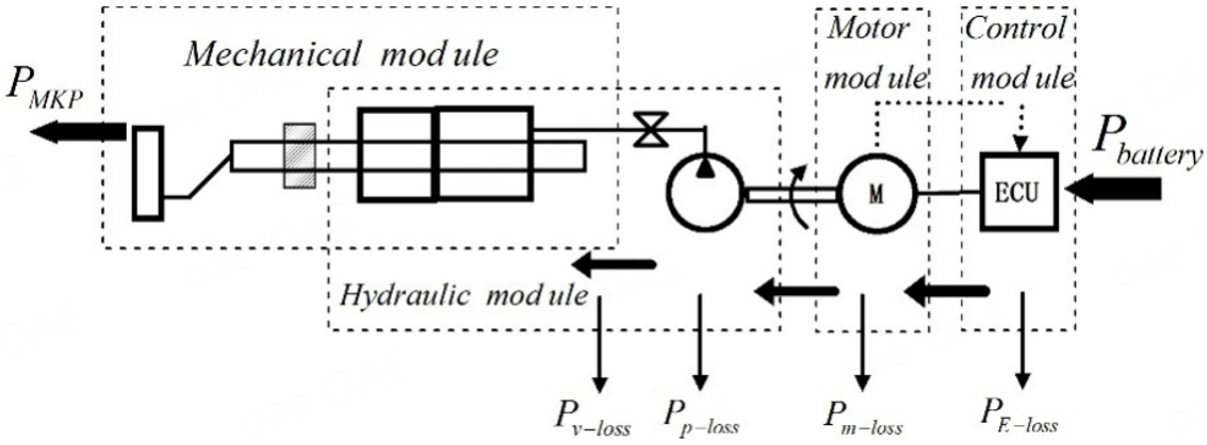

Figure 2. The schematic diagram of energy flow.

In this paper, the transfer function from the yaw velocity $\omega_r(S)$ to steering wheel $\theta_s(S)$ is defined as the steering sensitivity, expressed as

$$\frac{\omega_r(s)}{\theta_{sw}(s)} = \frac{\omega_r(s)}{\delta(s)} \frac{\delta(s)}{\theta_{sw}(s)} \tag{10}$$

Similar to steering road feel, the steering sensibility is also measured by the average frequency power in the range of 0-40 Hz and computed as

$$F_l = \frac{1}{2\pi\omega_0} \int_0^{\omega_0} \left| \frac{\omega_r(s)}{\theta_h(s)} \right|_{j=j\omega}^2 d\omega \tag{11}$$

2.2.3 Steering energy loss

Compared with traditional HPS systems, energy consumption of EHPS systems is greatly reduced. However, it still has a huge potential for energy saving. The schematic diagram of the energy flow of the EHPS system is shown in Figure 2.

The total energy of the steering system is supplied by the battery. One part of the energy is supplied to the ECU,and the energy loss is denoted as P_{E-loss}. The other part is supplied to the drive motor, which drives the hydraulic pump according to the ECU command. The energy loss of the drive motor is denoted as P_{m-loss}. The hydraulic pump pumps the hydraulic oil into rotary valve, and the energy losses of the two are denoted as P_{p-loss} and P_{v-loss}, respectively[9,14]. Thus, the total energy loss can be calculated as

$$P = P_{E-loss} + P_{m-loss} + P_{p-loss} + P_{v-loss} \tag{12}$$

where

$$\begin{cases} P_{E-\text{loss}} = R_a i^2 + \frac{U_s^2}{R_{\text{elec}}} \\ P_{m-\text{loss}} = \left[\frac{\frac{B_v n\pi}{30} + T_{Lo}}{K_a} r_a + \frac{k_e n\pi}{30} - K_a \omega(t) \right] i \\ P_{p-\text{loss}} = \frac{\rho}{8C_q^2} \left[\left(\frac{Q_S - A_P \dot{\theta} P r_P}{A_2} \right)^2 + \left(\frac{Q_S + A_P \dot{\theta} P r_P}{A_1} \right)^2 \right] (qn - Q_S) \\ P_{v-\text{loss}} = \frac{\rho}{8(C_q A_1)^2} \left(\frac{Q_s}{4} + A_p \frac{dx_r}{dt} \right)^3 + \frac{\rho}{8(C_q A_2)^2} \left(\frac{Q_s}{4} - A_p \frac{dx_r}{dt} \right)^3 \\ i = \frac{J_m}{K_a} \frac{d\omega(t)}{dt} + \frac{B_d}{K_a} \omega(t) + \frac{T_c}{K_a} \end{cases}$$

Table 1. The basic parameter of EHPS system

Name	Value	Name	Value
m/kg	4495	C_{21}/(N•m/rad)	14,130
m_s/kg	3350	C_{23}/(N•m/rad)	71,200
I_x/kg•m^2	2510	C_{a1}/(N•m•s/rad)	4,000
I_{xz}/kg•m^2	2810	C_{a1}/(N•m•s/rad)	3,800
I_z/kg•m^2	18800	d/m	0.23
k_1/(N/rad)	-2900	J_{sw}/kg•m^2	0.04
k_2/(N/rad)	-2900	C_q	0.62

Table 2. The initial value and range of each variable

Design variable	Initial value	Lower	Upper
A_p (m^2)	$1.2*10^{-4}$	$0.5*10^{-4}$	$2*10^{-4}$
p_b (m)	0.008	0.003	0.01
K_s (N/m)	80	30	150
J_m/kg•m^2	$5*10^{-3}$	10^{-3}	10^{-2}
r_p (m)	0.05	0.01	0.1
w (m)	10^{-3}	10^{-4}	$2*10^{-3}$

3. INTEGRATION OPTIMIZATION

As mentioned above, the optimization of EHPS system involves three evaluation indexes, steering road feel, steering sensitivity, and steering energy loss. Therefore, A multi-objective collaborative optimization model has been built, which simplifies the system decoupling, and the multi-objective optimization algorithm is applied to the model for a Pareto optimal solution set. Besides, the basic parameters of the EHPS system are shown in Table 1.

3.1. Optimization model

Based on collaborative optimization theory, the main system is divided into three independent subsystems, which is convenient for parallel computation and reduces the optimization time. In the main system, three optimization objectives, steering road feel, steering sensibility and energy loss, are optimized by multi-objective optimization algorithm. Besides, the consistency constraint of design parameters is taken as the optimization goal of each subsystem, and the sequential quadratic programming (NLPQL) algorithm is used to optimize each system.

In this paper, the effective area of piston A_p, the moment of inertia of motor J_m, the stiffness coefficient K_s, the stator thickness p_b, the gap width of rotary valve and the radius of the rack and pinion r_p are selected as the optimization variables. The initial value and design scope of each variable are given in Table 2.

The main system of optimization model is given by

$$\begin{cases} Minimize \quad P \\ Minimize \quad F_l \\ Maximize \quad S_c \\ Design \quad Variable \quad Bounds: \\ \qquad 3 \le T_p \le 5 \\ Z_L \le Z\left(A_p, p_b, K_s, J_m, r_p, w\right) \le Z_U \\ \qquad R_{1,2,3} \le 0.01 \end{cases} \tag{13}$$

where T_p is effective power torque, which is computed by

$$T_p = A_p r_p p_{ab} \tag{14}$$

where

$$\begin{cases} p_{ab} = \frac{\rho}{8\left(C_q A_{f2}\right)^2}\left(qn\eta_v - A_p r_p \dot{\theta}_p\right)^2 - \frac{\rho}{8\left(C_q A_{f1}\right)^2}\left(qn\eta_v + A_p r_p \dot{\theta}_p\right)^2 \\ A_{f1} = NL[w + R\left(\theta_z - \theta_p\right)] \\ A_{f2} = NL[w - R\left(\theta_t - \theta_p\right)] \end{cases}$$

The first subsystem named as energy loss is given by

$$\begin{cases} Minimize \\ R_1 = \left(1 - A'_p/A_p\right)^2 + \left(1 - p'_b/p_b\right)^2 \\ \quad + \left(1 - J_m/J'_m\right)^2 + \left(1 - r'_p/r_p\right)^2 + \left(1 - w'/w\right)^2 \\ Design \quad Variable \quad Bounds: \\ \quad 3 \le T'_p \le 5 \\ \quad x_L \le x\left(A'_p, p'_b, K'_s, J'_m, r'_p, w'\right) \le x_U \end{cases} \tag{15}$$

The second subsystem named as road feel is given by

$$\begin{cases} Minimize \\ R_2 = \left(1 - A''_p/A_p\right)^2 + \left(1 - p''_b/p_b\right)^2 \\ \quad + \left(1 - r''_p/r_p\right)^2 + \left(1 - J_m/J''_m\right)^2 + \left(1 - K''_s/K_s\right)^2 \\ Design \quad Variable \quad Bounds: \\ \quad 3 \le T''_p \le 5 \\ \quad x_L \le x\left(A''_p, p''_b, K''_s, J''_m, r''_p\right) \le x_U \end{cases} \tag{16}$$

The third subsystem named as steering sensibility is given by

$$\begin{cases} Minimize \\ R_3 = \left(1 - A'''_p/A_p\right)^2 + \left(1 - p'''_b/p_b\right)^2 + \left(1 - K'''_s/K_s\right)^2 \\ \quad + \left(1 - J'''_m/J_m\right)^2 + \left(1 - r'''_p/r_p\right)^2 + \left(1 - w'''/w\right)^2 \\ Design \quad Variable \quad Bounds: \\ \quad 3 \le T'''_p \le 5 \\ \quad x_L \le x\left(A'''_p, p'''_b, K'''_s, J'''_m, r'''_p, w'''\right) \le x_U \end{cases} \tag{17}$$

According to the above models, the multi-objective collaborative optimization model of EHPS is showed in Figure 3.

3.2. Multi-objective optimization algorithm

The NSGA-II algorithm has excellent global search performance and is often used in multi-objective optimization. On the one hand, the NSGA-II introduces an elite strategy in the process of ranking, which avoids the loss of non-dominated individuals in the evolution process and speeds up the convergence speed of the algorithm. On the other hand, the NSGA-II improves the crowded-comparison approach, which ensures the diversity of the next generation and enhances the global exploratory capability of the algorithm.

The main steps of NSGA-II algorithm can be depicted as follows.

(1) Generate the initial population P_0 at random and the size of P_0 is N;

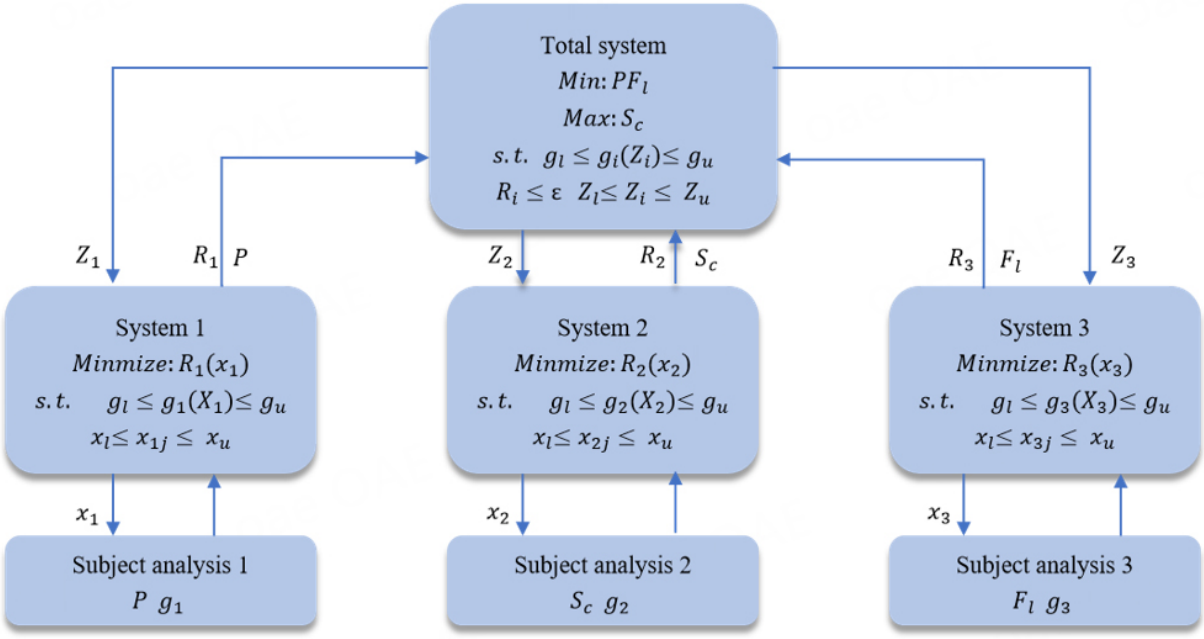

Figure 3. Optimization model of EHPS.

(2) Calculate the fitness degree of each individual by fitness function, sorting all individuals according to non-dominated regulation;

(3) Generate the next population $Q_t(t) \geq 1$ by crossover and mutation, and the size of Q_t is N. Forming a new population R_t consisted of P_t and Q_t;

(4) Calculate the fitness degree and crowd degree for each individual. Then, select N individuals to constitute a new population P_{t+1} according to the non-dominated regulation;

(5) $t = t + 1$;

(6) Run Step 3 to Step 5 repeatedly until t equals to the maximum generation.

The flowchart of the NSGA-II algorithm is shown in Figure 4.

3.3. Optimization results

According to the established multi-objective collaborative optimization model of the EHPS system, the NSGA-II is applied to the main system for the overall optimization of evaluation indexes, and the NLPQL algorithm is applied to each subsystem for the consistency of design variables. Additionally, the multi-objective particle swarm optimization algorithm (MOPSO) and NCGA multi-objective optimization algorithms are applied to the main system, and the NSGA-II algorithm is used to optimize the whole EHPS system. The solution set distribution of the optimization results is shown in Table 3, and the multi-objective optimization results are shown in Table 4.

Table 4 shows the distribution of the Pareto solutions obtained by different multi-objective algorithms. It should be noted that all algorithms are executed 2000 times.

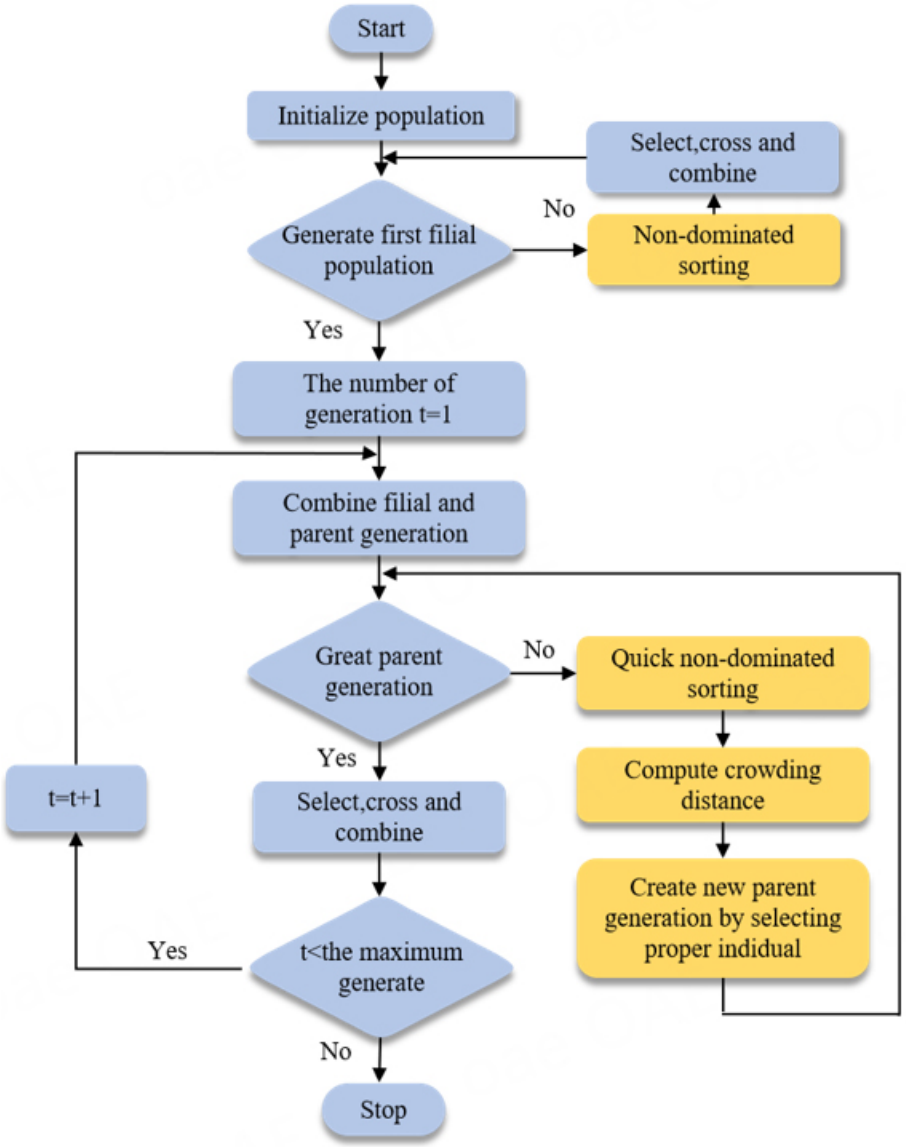

Figure 4. The flowchart of NSGA-II.

Firstly, multi-objective optimization method and multi-objective collaborative optimization method are compared. The distribution of the Pareto solutions obtained by only the NSGA-II is similar to the result by the NSGA-II with CO. 278 Pareto solutions are obtained by the NSGA-II with CO, and form a near-complete Pareto front. However, the number of Pareto solutions (104) obtained by the multi-objective optimization (NSGA-II) is too few to form a near-complete Pareto front. Furthermore, due to the insufficient number of solutions, poor non-dominant solutions cannot be eliminated, resulting in a low quality of the optimization solution set. Thus, it could be concluded that the multi-objective collaborative optimization has better solution set diversity and higher solution quality than the multi-objective optimization.

Secondly, the results obtained by CO combing with different multi-objective algorithms are compared. The MOPSO gets 53 Pareto solutions, while the NCGA and the NSGA-II have 269 and 278 Pareto solutions, respectively. Due to the neighborhood cultivation mechanism of the NCGA algorithm, excellent parent generations could be preserved in the next generation, which guarantees more Pareto solutions obtained, and the Pareto solutions distribution is more concentrated. In terms of NSGA-II algorithm, the elitist strategy is introduced;

Table 3. The distribution of Pareto solutions

	Pareto solutions
NSGA-II	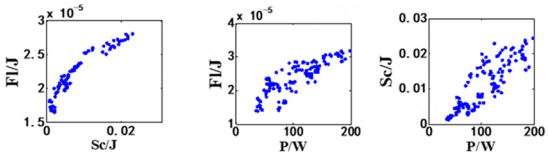
NSGA-II (CO)	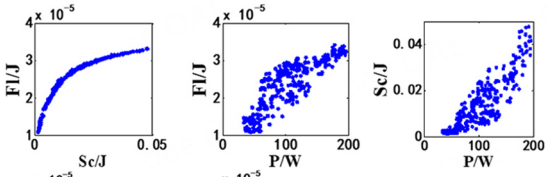
MOPSO (CO)	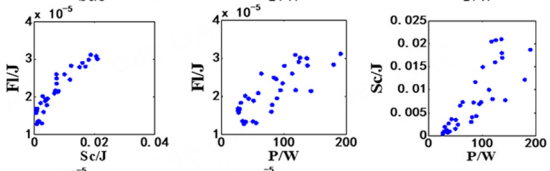
NCGA (CO)	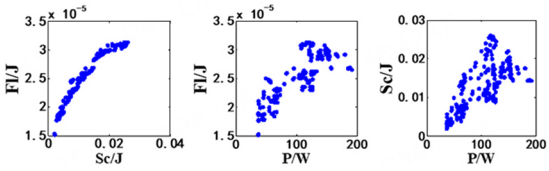

Table 4. Optimal result

Design variable	Initial value	NSGA-II	NSGA-II (CO)	MOPSO (CO)	NCGA (CO)
A_p (m^2)	$1.2*10^{-4}$	$1.21*10^{-4}$	$1.79*10^{-4}$	$1.24*10^{-4}$	$1.50*10^{-4}$
p_b (m)	0.008	0.0034	0.0044	0.0035	0.0042
K_s (N/m)	80	32.45	31.7	41.4	36.2
J_m (kg· m^2)	$6*10^{-3}$	$1.26*10^{-3}$	$1.82*10^{-3}$	$1.12*10^{-3}$	$1.78*10^{-3}$
r_p (m)	0.06	0.037	0.032	0.034	0.021
w (m)	10^{-3}	$5.88*10^{-4}$	$6.76*10^{-4}$	$5.59*10^{-4}$	$5.27*10^{-4}$
F_l (J)	$3.24*10^{-5}$	$2.81*10^{-5}$	$2.65*10^{-5}$	$2.61*10^{-5}$	$3.13*10^{-5}$
S_c (J)	0.016	0.023	0.027	0.021	0.026
P (W)	132.41	124.46	118.28	120.24	116.34

thus, excellent parent generations information could also be preserved in the next generation. Meanwhile, the sorting method based on crowding distance ensures that the Pareto solutions are distributed uniformly.

The optimization results are shown in Table 4. Through the multi-objective collaborative optimization method, the average frequency domain energy of steering sensibility is 2.65×10^{-5} J, which is decreased by 19.2% compared with the initial value. The average frequency domain energy of the steering road feel is 0.027 J, and it is 1.69 times bigger than the initial value. Moreover, the steering energy loss is reduced to 118.28 W, which is reduced by 10.8% compared to the initial value. Besides, compared to the results by only the NSGA-II algorithm, the optimization objectives have been further improved by the NSGA-II algorithm with CO. The average frequency domain energy of steering sensitivity is further reduced by 5.69%. The average frequency domain energy of the steering road feel is further increased by 17.39%, and the steering energy loss is further reduced by 5.00%. Furthermore, the optimization by the NSGA-II algorithm with CO has the best comprehensive performance compared with the results obtained by CO with the other two multi-objective algorithms.

The Bode diagram of the steering road feel step response is shown in Figure 5. The amplitude in the 0-40 Hz range has been improved compared to that before optimization. Especially for the NSGA-II with CO method, it gets the highest average frequency domain energy among the optimization algorithms, which means that

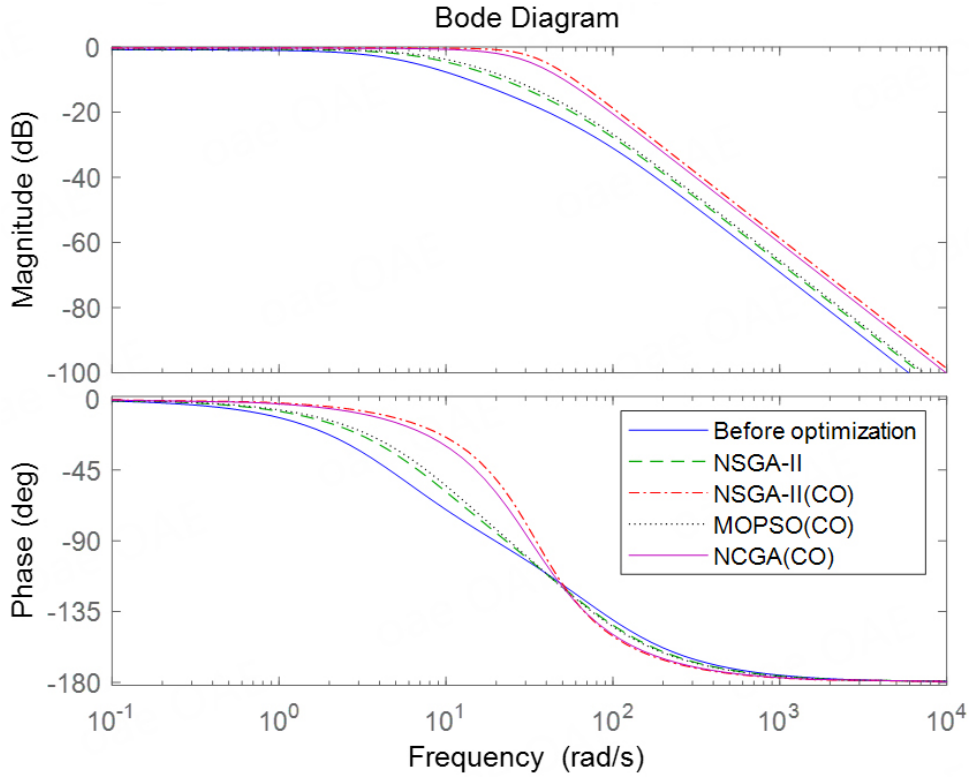

Figure 5. Step response Bode diagram of steering road feel.

the information from the 0-40 Hz range of the road surface can be transmitted to the driver better.

The Bode diagram of the steering sensibility step response is shown in Figure 6. Although the NSGA-II with CO method does not obtain the least steering sensibility, the optimization result obtained is still greatly improved compared to that before optimization.

Therefore, it could be concluded that multi-objective collaborative optimization can improve the steering road feel and reduce the steering sensitivity while improving the economy of the steering system. At the same time, the collaborative optimization of NSGA-II with CO has better solution sets diversity and comprehensive optimization results.

4. CONCLUSIONS

(1) On the basis of the EHPS system dynamics model and energy flow analysis, the evaluation index formula of the steering system is derived for the first time, including steering road feel, steering sensibility, and steering energy loss. In addition, considering the coupling relationship between subsystems, a multi-objective collaborative optimization model is established to achieve parallel computing.

(2) The multi-objective collaborative optimization further improves the performance of the EHPS system compared with the multi-objective optimization. Besides, the NSGA-II algorithm shows the best comprehensive performance in optimizing the design parameters of the EHPS system in the comparison of CO combing with multi-objective algorithms.

(3) The optimization results show that the EHPS system is optimized successfully and multiple evaluation in-

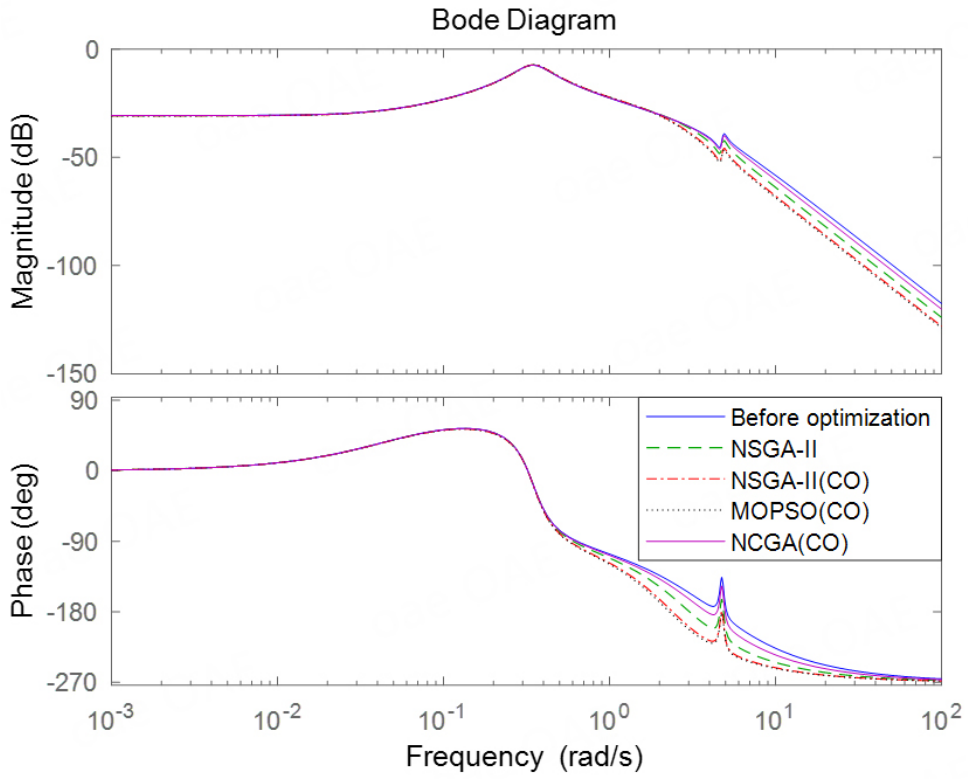

Figure 6. Step response Bode diagram of steering sensibility.

dexes could be improved simultaneously. Besides, the optimization is beneficial for promoting the application of the EHPS system in the area of power steering and also serves as a good example for the optimization of electric power steering systems and active steering systems.

DECLARATIONS

Acknowledgments

The authors would like to thank the reviewers for their thoughtful comments and efforts towards improving our manuscript.

Authors' contributions

Conceptualization: Cui T
Experiment and analyze data: Cui T, Wang S
Manuscript drafting: Cui T, Chen X
Manuscript edition and review: Cui T, Wang S, Qu Y, Chen X

Availability of data and materials

Not applicable.

Financial support and sponsorship

The research presented within this article is supported by the Fundamental Research Funds for the Central Universities (Grant No. Jz2021HGQA0286).

Conflicts of interest

All authors declared that there are no conflicts of interest.

Ethical approval and consent to participate

Not applicable.

Consent for publication

Not applicable.

Copyright

Appendix for Nomenclature

REFERENCES

1. Liu C, Wang C, Zhao W, Guo Z. Displacement characteristics hierarchical control of electro-hydraulic compound steering for commercial vehicle. *J Mech Eng Sci* 2022;236:6395-409. DOI
2. Guo ZQ, Wu HX, Zhao WZ, et al. Coordinated control strategy for vehicle electro-hydraulic compound steering system. *J Automot Eng* 2020;235:732-43. DOI
3. Du H, Zhang QM, Chen SM, et al. Modeling, simulation, and experimental validation of electro-hydraulic power steering system in multi-axle vehicles. *J Automot Eng* 2019;233:317-32. DOI
4. Zhang L, Wang Z, Ding X, Li S, Wang Z. Fault-tolerant control for intelligent electrified vehicles against front wheel steering angle sensor faults during trajectory tracking. *IEEE Access* 2021;9:65174-86. DOI
5. Ding X, Wang Z, Zhang L. Hybrid control-based acceleration slip regulation for four-wheel-independent-actuated electric vehicles. *IEEE Trans Transp Electrific* 2021;7:1976-89. DOI
6. Zhang L, Zhang Z, Wang Z, Deng J, Dorrell DG. Chassis coordinated control for full X-by-wire vehicles-a review. *Chin J Mech Eng* 2021;34:1-25. DOI
7. Du H, Wang L, Chen JD, et al. Adaptive fuzzy radial basis function neural network integral sliding mode tracking control for heavy vehicle electro-hydraulic power steering systems. *J Automot Eng* 2020;234:872-86. DOI
8. Lin L, Wang W, Liu ZQ. Modeling and simulation of slip frequency control for induction motor in electric vehicle EHPS system. *Appl Mech Mater*2014;635-7:1251-5. DOI
9. Kim SH, Min CS, Chong NC. Development of EHPS motor speed map using HILS system. *IEEE Trans Veh Technol* 2013;62:1553-67. DOI
10. Ye M, Wang Q, Jiao S. Robust H_2/H_∞ control for the electrohydraulic steering system of a four-wheel vehicle. *Math Probl Eng* 2014;4:1-12. DOI
11. Hur J. Characteristic analysis of interior permanent-magnet synchronous motor in electrohydraulic power steering systems. *IEEE Trans Industr Inform* 2008;55:2316-23. DOI
12. Cui TW, Zhao WZ, Wang CY. Parametric optimization of a steering system based on dynamic constraints collaborative optimization method. *Struct Multidiscipl Optim* 2020;61:787-802. DOI
13. Zhao WZ, Wang CY, Li YJ, et al. Integrated optimisation of active steering and semi-active suspension based on an improved memetic algorithm. *Int J Veh Des* 2015;67:388-405. DOI
14. Crews JH, Mattson MG, Buckner GD. Multi-objective control optimization for semi-active vehicle suspensions. *J Sound Vib* 2011;330:5502-16. DOI
15. Chen S, Shi T, Wang D, Chen J. Multi-objective optimization of the vehicle ride comfort based on kriging approximate model and NSGA-II. *J Mech Sci Technol* 2015;29:1007-18. DOI
16. Deb A, Srinivas GR, Chou CC. Development of a practical multi-disciplinary design optimization (MDO) algorithm for vehicle body design. *SAE Tech Pap* 2016;1:1537. DOI
17. Cui TW, Zhao WZ, Tai K. Optimal design of electro-hydraulic active steering system for intelligent transportation environment. *Energy* 2021;214:118911. DOI
18. Zhou PZ, Du JB, Lv ZH. Simultaneous topology optimization of supporting structure and loci of isolators in an active vibration isolation system. *Comput Struct* 2018;194:74-85. DOI
19. Zhao WZ, Wang YQ, Wang CY. Multidisciplinary optimization of electric-wheel vehicle integrated chassis system based on steady endurance performance. *J Clean Prod* 2018;186:640-51. DOI
20. Martins JRRA, Lambe AB. Multidisciplinary design optimization: a survey of architectures. *AIAA J* 2013;51:2049-75. DOI
21. Park EJ, Luz LFD, Suleman A. Multidisciplinary design optimization of an automotive magnetorheological brake design. *Comput Struct* 2008;86:207-16. DOI

22. Zadeh PM, Toropov VV, Wood AS. Metamodel-based collaborative optimization framework. *Struct Multidiscipl Optim* 2009;38:103-15. DOI
23. Zhou G, Ma ZD, Cheng A, et al. Design optimization of a runflat structure based on multi-objective genetic algorithm. *Struct Multidiscipl Optim* 2015;51:1-9. DOI
24. Huang H, An H, Wu W, Zhang L, Wu B, Li W. Multidisciplinary design modeling and optimization for satellite with maneuver capability. *Struct Multidiscipl Optim* 2014;50:883-98. DOI
25. Mitra AC, Patil MV, Banerjee N. Optimization of vehicle suspension parameters for ride comfort based on RSM. *J Inst Eng* 2015;96:165-73. DOI